

LIMITS TO THE PERFORMANCE OF THE LHC WITH ION BEAMS*

J.M. Jowett[#], H.H. Braun, M.I. Gresham^{*}, E. Mahner, A.N. Nicholson, E. Shaposhnikova,
CERN, Geneva, Switzerland

I.A. Pshenichnov, INR, Russian Academy of Sciences, Moscow, Russia

Abstract

The performance of the LHC as a heavy-ion collider will be limited by a diverse range of phenomena that are often qualitatively different from those limiting the performance with protons. We summarise the latest understanding and results concerning the consequences of nuclear electromagnetic processes in lead ion collisions, the interactions of ions with the residual gas and the effects of lost ions on the beam environment and vacuum. Besides these limitations on beam intensity, lifetime and luminosity, performance will be governed by the evolution of the beam emittances under the influences of synchrotron radiation damping, intra-beam scattering, RF noise and multiple scattering on residual gas. These effects constrain beam parameters in the LHC ring throughout the operational cycle with lead ions.

INTRODUCTION

The design parameters of the LHC as a lead ($^{208}\text{Pb}^{82+}$) ion collider are given in [1] and [2]. There are two sets: the “Nominal Scheme” with target luminosity $L \approx 10^{27} \text{ cm}^{-2}\text{s}^{-1}$ and the “Early Scheme” [2,9] with 10 times fewer bunches and higher β^* at the collision points but the same number of particles, $N_b \approx 7 \times 10^7$, per bunch.

BEAM-BEAM INTERACTIONS

Conventional beam-beam effects are relatively weak for ions compared to protons; see [2] for further discussion of their role in the beam-separation scheme.

Photo-nuclear interactions in beam-beam collisions, including Bound-Free Pair Production (BFPP, called ECPP in [1]), in which an e^+e^- pair is created with the electron bound to one of the colliding nuclei, and Electromagnetic Dissociation (ED) are the dominant sources of particle loss from the beam [1]. Moreover BFPP directly limits luminosity because the secondary beam of Pb^{81+} ions emerging from the interaction point creates a concentrated heat-loss in a cryo-dipole that may then quench [3,1,2].

Beam-Screen Description and Loss Localisation

The calculation of the distribution of Pb^{81+} ions on the beam screen has been refined from the simple model of [3] and the Twiss-function based calculation of [1]. While thin-lens tracking of ions is implemented in the

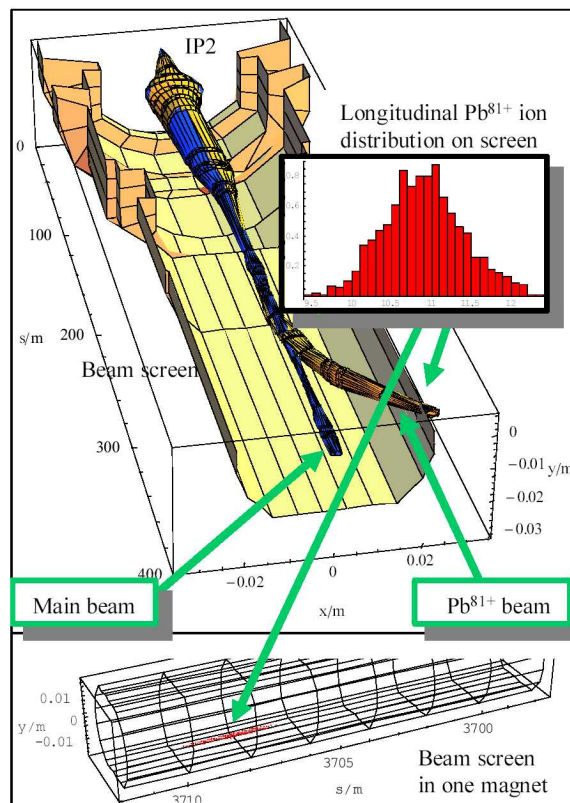


Figure 1: Main beam of Pb^{82+} and the secondary beam of Pb^{81+} emerging from IP2 (top of picture). The 5σ envelopes of the beams are shown inside the beam screen in the usual beam coordinate system (x, y, s) . The Pb^{81+} beam hits the screen about 350m downstream in a dispersion suppressor dipole magnet.

MAD program, this only checks for loss of a particle at the end of each element for which an aperture (the beam-screen in the LHC case) has been defined. This is not, in general, sufficient even to correctly determine the element in which particles are lost. To overcome these limitations, we have extended MAD’s tracking in the Madtomma framework [5] of Mathematica packages. The new package makes an intelligent extension of the discrete aperture description of MAD with continuous functions (avoiding the brute-force approach of inserting many thousands of aperture-bearing marker elements in the LHC element sequence). It can then correctly locate the element in which particles are lost and perform a fast analytical calculation of the intersections of the incoming particle trajectories with the three-dimensional beam-screen geometry in that element. This works by

* Summer Student from Reed College, Portland, Oregon, USA.

[#] John.Jowett@cern.ch

subsuming all beam screen types occurring in the LHC into a single sufficiently general type (the ‘‘RECTELLIPSE’’) and solving a system of equations embodying the thick-lens linear optics and 3D geometry of the beam screen.

An example of the results, showing the distribution of the secondary beam of Pb^{81+} ions on the beam screen downstream from the ALICE experiment at IP2 is shown in Figure 1. The shape of the secondary beam is drastically modified (with respect to that of the main beam) by the uncorrected chromatic effects of the low- β insertion, increasing the longitudinal density of energy deposition. Together with the new calculations of ED and NF processes currently being implemented in the FLUKA program (see also [6]), these results will shortly allow more refined estimates of the heat-deposition and quench limit for the environment of beam-screen and superconducting magnets. Present estimates are that the energy deposition exceeds the quench limit by about a factor 2 at nominal luminosity.

BEAM-ENVIRONMENT INTERACTIONS

Collimation

The fundamental hadronic and ED interactions of lost ions with the material of the collimator system lead to a class of serious limitations on the total ion *current* that can be stored; see the separate paper [6]. In terms of luminosity, these limits occur at a level similar to those described above.

Beam-Vacuum Interactions

Table 1 shows the components of the total cross-section $\sigma_{bg} = \sigma_n + \sigma_{ED}$ for the Pb beam interacting with residual gases; the hadronic part σ_n is given by abrasion-ablation calculations [10] and the ED part σ_{ED} by RELDIS [11].

Table 1: ED and hadronic cross-sections for Pb ions of energy 2.75A TeV impinging on residual gas molecules

	H ₂	He	CH ₄	H ₂ O	CO	CO ₂
σ_n / barn	4.2	2.9	12.0	8.0	7.5	11.3
σ_{ED} / barn	0.03	0.2	1.9	3.3	5.1	8.3

They are some 20-50 times larger than the corresponding values for protons leading to correspondingly more stringent vacuum requirements. Detailed evaluations of residual gas density for ion beams in the LHC have not yet been made. However, with rather pessimistic assumptions (the average residual gas densities in the whole ring taken to be $\frac{1}{4}$ of the ‘‘startup’’ vacuum conditions for proton beams in the insertions [12]), these lead to an intensity lifetime

$$\tau_{bg}^{-1} = \left(\sum_g n_g \sigma_{bg} \right) v_b \approx (80 \text{ h})^{-1} \quad (1)$$

where v_b is the beam velocity. Multiple scattering of beam particles on the residual gas leads to a linear growth

of the emittance with time. Calculations (extending [7] to ions) depend quite strongly on the gas density distribution weighted with the β -functions, in particular the density of CO and CO₂ in the interaction regions. The time taken for the emittance to increase by its design value varies from ~ 1 h in start-up conditions to >100 h in a well-conditioned chamber. Better estimates of residual gas density are required to eliminate this as a serious concern.

Molecular Desorption

Losses of ions on the vacuum chamber are a mechanism for vacuum degradation by means of molecular desorption. Concerns that the desorption coefficient might increase dramatically with the energy of incident ions have been addressed by a programme of measurements at the SPS [8] with the reassuring result that this effect is not expected to be a major limitation of ion operation at the LHC.

BEAM AND LUMINOSITY LIFETIME

The LHC will be the first heavy-ion collider for which synchrotron radiation damping has significant effects on beam dynamics [2].

The longitudinal emittance (per charge) injected from the SPS into the LHC has been reduced [2] to $\varepsilon_l = 0.7$ eVs because the use of a 200 MHz capture RF system is no longer foreseen. To avoid strong IBS at higher energy, a controlled blow-up to $\varepsilon_l = 2.5$ eVs will be carried out during the ramp to collision energy.

Estimates of the luminosity evolution during a fill are made by solving the set of non-linear coupled ordinary differential equations for the emittances and intensities of the beams [14]. For purposes of illustration, we simplify here by considering the degenerate case where all bunches of both beams have identical ε_l , intensity (N_b ions per bunch) and horizontal emittance $\varepsilon_x = \beta_x \sigma_x$ and assume (somewhat pessimistically) that residual betatron coupling maintains the round beam condition, $\varepsilon_y \approx \varepsilon_x$, as a slaving relationship, on shorter time scales

$$\begin{aligned} \dot{N}_b(t) &= - \left(\sum_g n_g \sigma_{bg} \right) v_b N_b(t) - \frac{\sigma_{\text{tot}} n_{\text{exp}} f_0 N_b(t)^2}{4\pi\beta^* \varepsilon_x} \\ \dot{\varepsilon}_x(t) &= \frac{\varepsilon_x(t)}{T_{\text{IBSx}}(N_b, \varepsilon_x(t), \varepsilon_l(t))} - \frac{2\varepsilon_x(t)}{\tau_x} \\ \dot{\varepsilon}_l(t) &= \frac{\varepsilon_x(t)}{T_{\text{IBSl}}(N_b(t), \varepsilon_x(t), \varepsilon_l(t))} - \frac{4\varepsilon_l(t)}{\tau_x} + D_{\text{RF}}(t) \end{aligned} \quad (2)$$

where n_{exp} is the number of experiments illuminated, τ_x is the radiation damping time, σ_{tot} is the total cross-section [1] for ion removal in collisions, T_{IBSx} and T_{IBSl} are functions giving the IBS growth times (evaluated for the complete LHC collision optics using the implementation of the theory of [13] in [4]), $D_{\text{RF}}(t)$ represents diffusion

due to RF noise and other symbols have their customary meanings [2]. It is assumed that the dispersion at the RF cavities is well enough corrected that the transverse blow-up from RF noise can be neglected. Similarly for multiple scattering on residual gas (see above). The betatron damping time for ϵ_x is $\tau_x/2 \approx 12.6$ h, half the value for protons [2].

The upper set of curves in Figure 2 shows what would happen if there were no radiation damping: after a few hours, the emittance would exceed the acceptance, because of IBS, leading to beam losses. In reality, at the beginning of a fill with nominal intensity, radiation damping essentially cancels out the IBS. However the more rapid damping of ϵ_l tends to increase $1/T_{IBSx}$ and this can be countered by a $D_{RF} > 0$. Intensity losses from luminosity finally reduce the IBS to the point where the emittance can steadily shrink. Thus, efficient luminosity operation of the LHC with lead ion beams will only be possible thanks to radiation damping. Figure 3 provides another example of the essential role of radiation damping: the evolution of emittance and luminosity from the nominal initial parameters is compared with a situation identical except for a 20% larger initial emittance, possibly created by errors in the ramp. Thanks to the lower initial luminosity, the intensity lasts longer while the emittance damps. Eventually the luminosity overtakes that of the nominal beam. The loss of integrated luminosity for a given length of store (> 2 h) is much less than 20%.

CONCLUSIONS

The luminosity of Pb-Pb collisions in the LHC will be directly limited by BFPP-induced magnet quenches. The beam current will be limited by collimation efficiency. Radiation damping plays an essential role in countering the effects of intra-beam scattering and minimising the consequences of any emittance degradation during the ramp. Vacuum requirements for lead ions are much more stringent than for protons. Emittance blow-up by multiple scattering on residual gas is potentially a serious limit but cannot be estimated until the vacuum conditions with lead ions are better known.

Acknowledgements: We thank K. Schindl and many other colleagues for profitable discussions.

REFERENCES

- [1] J.M. Jowett et al, "Heavy Ion Beams in the LHC", PAC2003.
- [2] The LHC Design Report, Vol. I The LHC Main Ring, CERN-2004-003 Chapter 21 and references therein.
- [3] S.R. Klein, Nucl. Inst. & Methods **A 459** (2001) 51.
- [4] The MAD program, <http://cern.ch/mad>.
- [5] Madtomma, <http://cern.ch/jowett/Madtomma>.
- [6] H.H. Braun et al, this conference.
- [7] N. Mokhov, V.I. Balbekov, in Handbook of Accelerator Physics and Engineering, (Eds. A.W. Chao, M. Tigner), World Scientific 1999.

- [8] E. Mahner et al, this conference.
- [9] K. Schindl et al, this conference.
- [10] J.-J. Gaimard et al, Nucl. Phys. **A531** (1991) 709.
- [11] I.A. Pshenichnov et al, Phys. Rev. **C64** (2001) 024903
- [12] A. Rossi et al, LHC Project Report 674 (2003).
- [13] J.D. Bjorken, S. Mtingwa, Part. Accel. **13** (1983) 115
- [14] J.M. Jowett, A.N. Nicholson, to be published.

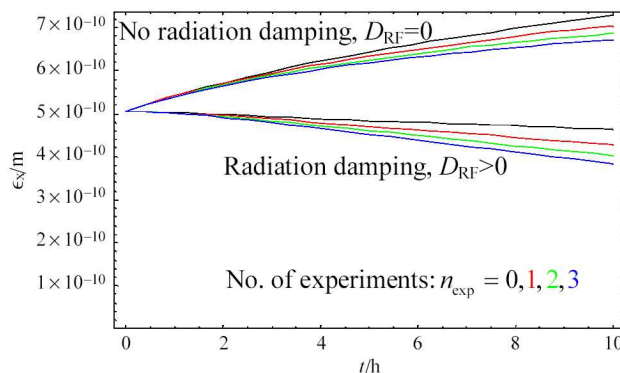


Figure 2: Effect of radiation damping on emittance starting from the nominal beam parameters. The lower set curves have D_{RF} chosen to increase ϵ_l to 3 eV s over the first two hours.

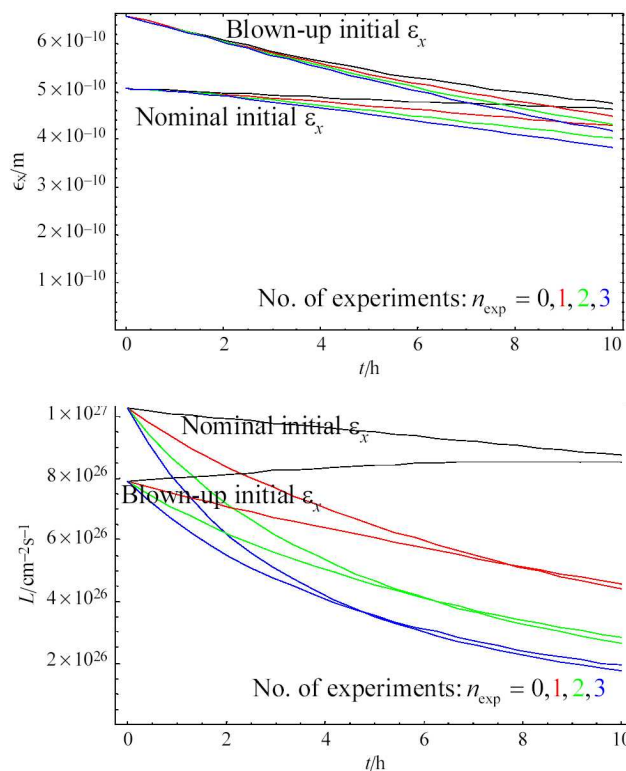


Figure 3: Evolution of emittance and luminosity, starting from the nominal parameters, except that in one set of curves, the initial emittance is increased by 20%.